Pacific Graphics (2017)
J. Barbic, W.-C. Lin, and O. Sorkine-Hornung (Editors)

Short Paper

Adaptive Measurement of Anisotropic Material Appearance

R. Vávra† and J. Filip

Institute of Information Theory and Automation of the CAS, Czech Republic

Abstract

We present a practical adaptive method for acquisition of the anisotropic BRDF. It is based on a sparse adaptive measurement of the complete four-dimensional BRDF space by means of one-dimensional slices which form a sparse four-dimensional structure in the BRDF space and which can be measured by continuous movements of a light source and a sensor. Such a sampling approach is advantageous especially for gonioreflectometer-based measurement devices where the mechanical travel of a light source and a sensor creates a significant time constraint. In order to evaluate our method, we perform adaptive measurements of three materials and we simulate adaptive measurements of ten others. We achieve a four-times lower reconstruction error in comparison with the regular non-adaptive BRDF measurements given the same count of measured samples. Our method is almost twice better than a previous adaptive method, and it requires from two- to five-times less samples to achieve the same results as alternative approaches.

Categories and Subject Descriptors (according to ACM CCS): I.3.7 [Computer Graphics]: Three-Dimensional Graphics and Realism—Color, shading, shadowing, and texture I.4.1 [Computer Graphics]: Digitization and Image Capture—Reflectance

1. Introduction

Realistic appearance of spatially homogeneous materials is usually represented by means of a bidirectional reflectance distribution function (BRDF) as introduced in [NRH*77]. Precise measurement of the BRDF is time demanding due to the very high number of samples of the function that have to be taken. In this paper, we introduce a method for the adaptive measurement of the BRDF that provides precise results using even the limited number of samples. The method does not require any database of already measured materials and is well scalable; therefore, it can be used in every application where precision is important. We build upon the paper [FVH*13] that measures the BRDF by one-dimensional slices and we substantially extend its contributions.

Let us remind that the BRDF is a four-dimensional vector-valued function $f_r(\theta_i, \theta_v, \varphi_i, \varphi_v)$ of the illumination direction $\omega_i = [\theta_i, \varphi_i]$ and the viewing direction $\omega_v = [\theta_v, \varphi_v]$ that defines how light is reflected from a material. The three-dimensional simplification of the BRDF is called the isotropic BRDF and it can represent only a subclass of spatially homogeneous materials as, e.g., plastics or paints. In contrast, the full-dimensional BRDF is described as anisotropic. Anisotropic materials have variable reflectance when rotated around a surface normal and are common for many real-world materials that contain directional elements such as, e.g., thread in fabric or grain in wood.

The proposed method is based on our findings of typical behavior of anisotropic BRDFs. We assume that each two-dimensional BRDF subspace of fixed θ_i, θ_v (see Fig. 1) and its important features can be captured by several diagonal and anti-diagonal cross-sections (so-called *slices*). Sampling the BRDF subspace only along the slices saves huge amount of samples (see [FVH*13]). Another saving is done by choosing only certain subspaces (e.g., by limitation of values of θ_i, θ_v to multiples of 15°, see Fig. 2-left). Then, elevation-dependent behavior is captured by another type of slices (see Fig. 2-right). The slices form a sparse 4D structure in the BRDF space. Their ability to capture important features of the BRDF depends on their density. Although all the values along the structure itself present substantial reduction of BRDF samples when compared to a dense regular sampling, we need to reduce the number of measured values even more to make the method practical. That is done by a sparse but adaptive sampling along individual slices, i.e., one-dimensional signals.

The main contribution of the paper is, to our best knowledge, introduction of the first adaptive method for precise measurement of the complete 4D anisotropic BRDF which does not rely on a database of already measured materials once the parameters of the method are identified.

2. Related Work

Methods for adaptive measurement and data interpolation are closely related, as our task is to reconstruct an unknown function well by a proper placement of novel samples based on previously measured values. Such a placement depends on the chosen interpolation method. Good candidates are global interpolation methods based on Radial Basis Functions (RBF) or Kriging [PTVF92].

† vavra@utia.cas.cz

DOI: 10.2312/pg.20171316

Although it seems that these methods might solve the problem of adaptive sampling in measurement of material appearance, they have high computational demands which become intractable when the number of samples exceeds several thousands. Adaptive measurement of material appearance is investigated in [FBLS07]; however, only in two dimensions. An adaptive approach for image-based BRDF measurement is proposed in [LLSS03] with planning of viewing and illumination directions based on minimization of uncertainty of analytical model parameters. Nauyoks et al. [NFM14] fit six isotropic BRDF models to the measured data. They iteratively add new samples by including illumination and viewing directions where the models differ the most.

Matusik et al. [MPM03] represent isotropic BRDFs using a wavelet basis or linear combination of the BRDFs. Similarly, Noll et al. [NKS14] represent the same BRDFs using basis functions; however, deviations of their reconstruction from the reference are approximated by a basis of correction functions. Nielsen et al. [NJR15] present an approach to reconstruct isotropic BRDFs from basis functions using extremely sparse measurements and Vavra and Filip [VF16b] extend their approach to anisotropic BRDFs. Majority of these approaches optimize a set of appropriate directional samples based on information in a database; however, they do not achieve any adaptivity towards the measured materials. As a result, they cannot measure materials with features not present in the database precisely enough.

None of the methods above provides a reliable way of effective acquisition of dense BRDF data without knowledge of previously recorded BRDFs. On the other hand, several interpolation methods applicable to measured samples exist. For instance, the barycentric interpolation [Cox69] or thin plate splines [Boo89]. Recently, Ward et al. [WKB14] reconstructed uniformly sampled BRDF measurements by RBFs interpolated using mass-transport solution. As these interpolation methods differ in quality and speed, we tested several of them and selected two as a reference for evaluation of the proposed approach of adaptive measurement.

Our paper builds on the paper [FVH*13] that uses slices to capture main features of 2D subspaces of the BRDF. Values on the slices are measured adaptively to minimize their number. Although individual subspaces can be captured very precisely, the whole BRDF is obtained using a simple interpolation and is therefore rather approximate. In this paper, we introduce two new types of the slices that enable us to capture all important features and to achieve better quality of reconstruction of the BRDF. Moreover, we study the optimal placement of the slices.

3. Introduction to One-Dimensional BRDF Slices

The BRDF is the four-dimensional vector-valued function of the elevation angles θ_i, θ_v and the azimuthal angles φ_i, φ_v. To enable efficient sampling of the entire BRDF, we propose to use four types of one-dimensional *slices*. Two of them, *axial* and *diagonal* slices, were introduced in [Fil12], where only one slice of each type per 2D BRDF subspace is used. We propose to use up to dozens of slices per subspace to capture the most of subtle details of the BRDF. Moreover, we suggest extending the concept to additional *horizontal* and *vertical* slices.

Axial and diagonal slices take place in the 2D BRDF subspaces defined by fixed θ_i and θ_v. These slices are designed to optimize

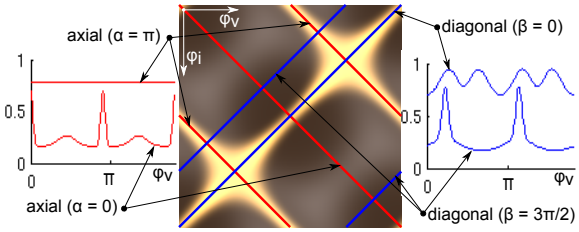

Figure 1: *A schema of axial (red, perpendicular to anisotropic highlights) and diagonal (blue, perpendicular to specular highlights) slices placed in the 2D subspace (fixed both $\theta_i = 60^\circ$ and $\theta_v = 60^\circ$) and their function values. Note that the subspace is periodical. Material* fabric112.

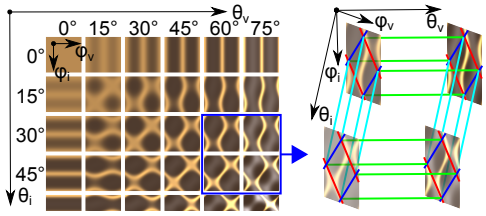

Figure 2: *A preview of a BRDF with highlighted axial (red), diagonal (blue), horizontal (green) and vertical (cyan) slices. Material* fabric112.

capture of specular reflections and anisotropic reflections. Axial slices s_A (red in all figures) are perpendicular to anisotropic reflections and diagonal slices s_D (blue in all figures) are perpendicular to specular reflections (see Fig. 1):

$$s_{A,\theta_i\theta_v\alpha}(\varphi_v) = f_r(\theta_i, \theta_v, \varphi_i = \varphi_v - \alpha, \varphi_v),$$
$$s_{D,\theta_i\theta_v\beta}(\varphi_v) = f_r(\theta_i, \theta_v, \varphi_i = \beta - \varphi_v, \varphi_v),$$

where α or β determines position of the slice in the 2D subspace chosen by elevation angles θ_i, θ_v. Each subspace is typically measured using several axial and several diagonal slices to accurately capture all reflections and their shape (see Fig. 1).

Horizontal and vertical slices are 1D subspaces of the BRDF. They are designed to capture change of reflectance values when the viewing elevation angle θ_v (horizontal slice, green) or the illumination elevation angle θ_i (vertical slice, cyan) is changed while other parameters are fixed as show in Figure 2-right:

$$s_{H,\theta_i\varphi_i\varphi_v}(\theta_v) = f_r(\theta_i, \theta_v, \varphi_i, \varphi_v),$$
$$s_{V,\theta_v\varphi_i\varphi_v}(\theta_i) = f_r(\theta_i, \theta_v, \varphi_i, \varphi_v).$$

Each horizontal or vertical slice passes through the intersection of axial and diagonal slices at all sampled elevations (e.g., 0^o, 15^o, 30^o, 45^o, 60^o, 75^o). Note that due to Helmholtz reciprocity, values of corresponding horizontal and vertical slices are equal, i.e., $s_{H,\theta_i\varphi_i\varphi_v}(\theta_v) = s_{V,\theta_i\varphi_v\varphi_i}(\theta_v)$. So only, e.g., horizontal slices need to be measured. All the four types of slices represent the sparse 4D structure in the four-dimensional BRDF space that effectively captures the main visual features of the measured BRDF (see Fig. 2-right). Each slice can be interpreted as an unknown one-dimensional signal that we need to measure and reconstruct. In case of the axial or diagonal slice the signal is periodic with the period of 360°. For adaptive placement of samples we use an enhanced version of the heuristic algorithm which was first introduced in [FVH*13] (see the supplementary material).

Once the measurement is done, we can reconstruct values of the four-dimensional BRDF by the method introduced in [FVH*13]. In the supplementary material, we show how to rewrite their equations to make transition to four dimensions possible. Also, we provide there equations for reconstruction of the desired value in the four dimensional space, and we describe implementation of the equations on graphics hardware.

4. A Study on the Optimal Placement of the Slices

Though values along individual slices are measured adaptively, positions of the slices in the BRDF space must be known in advance. Here we investigate which placement of the slices is optimal with respect to a given count of samples. Due to the insufficient number of available anisotropic BRDF measurements of high angular density and high accuracy, we perform a study on ten materials represented by the analytical BRDF model of Kurt et al. [KSKK10], which is one of state-of-the-art models for the anisotropic BRDFs. We selected ten materials, four of them measured in [NDM05] and the remaining materials come from our own measurements. All of the materials are anisotropic and include fabrics, brushed aluminum, and raw wood. Their fitted BRDFs are shown in Fig. 3 and the model parameters are included in the supplementary material.

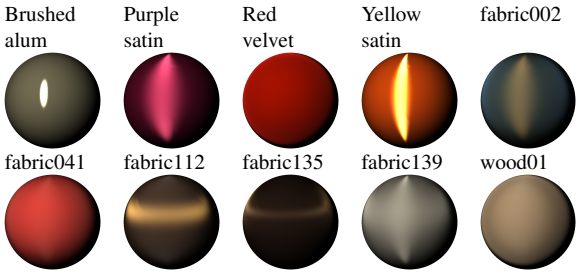

Figure 3: *Ten tested materials represented by the BRDF model [KSKK10] rendered on spheres.*

Placement Theory – The axial and diagonal slices are placed into 2D subspaces selected by θ_i and θ_v. The most straightforward approach is to deploy the slices regularly into the subspaces using:

$$\alpha,\beta \in \{k \cdot a_s; k \in \{0,1,\ldots,a_n-1\}, a_n = 2\pi/a_s\} \quad ,$$

where a_n is a count of the slices of one type in one subspace and a_s is the *azimuthal step* between two consecutive slices. Only parameter a_s has to be chosen. Let us denote that the position of the axial and diagonal slices might be chosen arbitrarily, but for simplicity, we limited ourselves to the regular distribution of both types of slices by one common step parameter.

Similarly, 2D subspaces are selected by one parameter called *elevation step* e_s as:

$$\theta_i,\theta_v \in \{k \cdot e_s, \theta_{max}; k \in \{0,1,\ldots,e_n-2\}\} \quad ,$$

where $e_n = \lceil \theta_{max}/e_s \rceil + 1$ is a count of elevations involved and θ_{max} is the maximal elevation. Measured subspaces are those resulting from all combinations of θ_i,θ_v. Finally, the horizontal and vertical slices are placed through all intersections of the axial and diagonal slices (see Fig. 2) to enable fast data interpolation using method [FVH*13].

An Analysis of the Optimal Placement – We perform an experiment to determine the optimal positions of the slices based on a user-defined count of samples n. We use all the ten BRDFs and compute their reconstructions for various combinations of the *azimuthal step* a_s, the *elevation step* e_s and the count of samples n. To make the precalculation computationally feasible, we restrict a resolution of the reconstructed BRDFs to 2^o and we use the maximal elevation angle $\theta_{max} = 80^o$ due to the unstable fitting of the BRDF by the analytical model for high elevation angles. Values of the *azimuthal step* parameter are $a_s \in \{12^\circ, 20^\circ, 36^\circ, 60^\circ, 180^\circ\}$, and values of the *elevation step* parameter are $e_s \in \{6^\circ, 8^\circ, 10^\circ, 12^\circ, 14^\circ, 16^\circ, 20^\circ, 28^\circ\}$. In total, we perform 20,646 simulated measurements and reconstructions of BRDFs, which consume over 20 days of computation time using four cores of Intel Xeon E5-2643 3.3GHz. To evaluate quality of the reconstructed BRDFs for the tested values of the parameters, we compute the Mean Relative Error (MRE) between the reference BRDF $f_r(\theta_i,\theta_v,\varphi_i,\varphi_v)$ and its reconstruction $f'_r(\theta_i,\theta_v,\varphi_i,\varphi_v)$:

$$MRE = \frac{1}{N} \cdot \sum_{\lambda,\theta_i,\theta_v,\varphi_i,\varphi_v} \frac{|f_{r_\lambda} - f'_{r_\lambda}|}{f_{r_\lambda}} \cdot 100[\%],$$

where $N = |\lambda| \times |\theta_i| \times |\theta_v| \times |\varphi_i| \times |\varphi_v|$ is the count of data points and $\lambda \in \{R,G,B\}$ is a color channel. Individual color channels are treated separately and the results are then summed up. We compute graphs of the MRE as a function of the number of adaptive samples n. As a result, there are $|a_s| \times |e_s| \times |m| = 5 \times 8 \times 10 = 400$ graphs $err_{m,a_s,e_s}(n)$, where m stands for one of 10 materials. Each graph captures the reconstruction error for a large range of samples n. In Figure 4 are plotted some of those graphs averaged across all the materials. The first group of graphs (a) shows progress of the error for the fixed parameter $e_s = 14^o$ and various values of the a_s parameter. The second group (b) shows the progress for the fixed parameter $a_s = 20^o$ and various values of the e_s parameter. Note that the fast convergence of individual graphs confirms efficiency of the adaptive sampling algorithm. From the graphs, it could be possible to conclusively select the best combination of the a_s, e_s parameters for a selected count of samples n relative to a given material m. Unfortunately, these selections are not unique across different materials as they exhibit individual behavior with respect to changes in the azimuthal and elevation angles. Therefore, we estimate the

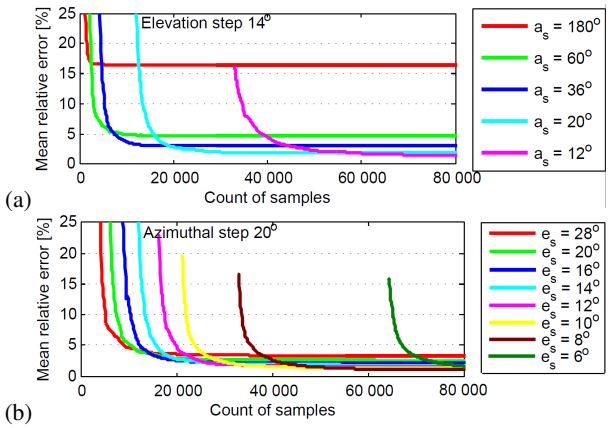

Figure 4: *The MRE of the reconstructed BRDF as a function of the count of samples averaged across all materials (a) for five values of the azimuthal step with the fixed value of $e_s = 14^\circ$ and (b) for eight values of the elevation step with the fixed value of $a_s = 20^\circ$.*

Table 1: *The optimal values of the a_s, e_s parameters depending on the demanded count of samples.*

$n \leq$	e_s	a_s	$n \leq$	e_s	a_s
667	28°	180°	17 096	12°	36°
932	20°	180°	20 969	10°	36°
1 034	16°	180°	22 291	8°	36°
1 060	28°	60°	33 879	12°	20°
2 272	20°	60°	38 735	10°	20°
3 230	16°	60°	79 469	8°	20°
4 928	14°	60°	184 655	6°	20°
5 645	16°	36°	∞	6°	12°
9 660	14°	36°			

optimal values $\widehat{a_s}, \widehat{e_s}$ of the parameters for a given count of samples n in a way that the sum of the errors across all the materials relative to the achievable error is minimized:

$$(\widehat{a_s}, \widehat{e_s})(n) = \underset{(a'_s \in a_s, e'_s \in e_s)}{\arg\min} \sum_{m=1}^{|m|} \frac{err_{m,a'_s,e'_s}(n)}{\min\limits_{(a''_s \in a_s, e''_s \in e_s)} err_{m,a''_s,e''_s}(n)}. \quad (1)$$

The resulting optimal values of the a_s, e_s parameters are summarized in Table 1. When a new material is measured, a user selects the parameters from the table and the method does not rely on any database anymore.

5. Results

This section presents results of the proposed method. First, due to lack of reliable densely measured BRDF data, we use synthetic data generated by the BRDF model (see Fig. 3). Thus, we can easily and quickly obtain a BRDF value of any direction and results of the experiment are not influenced by errors caused by a measurement process. To evaluate performance of the method on real data, we use a 3D scene and measure all the data needed to visualize the scene by a gonioreflectometer. Finally, we compare our method with the previous adaptive method [FVH*13].

Simulated Measurement Experiment – We evaluate performance of the proposed method in comparison with the uniformly distributed samples, which are taken at directions according to one of the thirty sampling schemes we designed (see the supplementary material). These schemes produce in total from $n = 435$ to $n = 354,061$ reciprocal samples. Values of the samples are interpolated using the barycentric [Cox69] or the RBF [PTVF92] interpolation. Notice that the second method is global while the first one is local and is therefore suitable for fast rendering on a GPU. Both methods compute results separately in each color channel. We interpolate the BRDF to a four-dimensional array using a uniform step of 2^o and the maximal elevation is 80^o, i.e., dimensions of the array are $|\theta_i| \times |\theta_v| \times |\varphi_i| \times |\varphi_v| = 41 \times 41 \times 180 \times 180$.

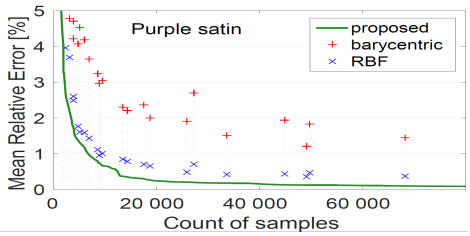

Figure 5: *The MRE as a function of the count of samples for material* purple satin.

To evaluate quality of the reconstructed BRDF, we compute the MRE between the reference BRDF and its reconstruction in $N = 3 \times 41 \times 41 \times 180 \times 180 = 163,393,200$ data points. The average decrease of the MRE due to usage of the proposed method instead of the barycentric interpolation or the RBF interpolation across all counts of samples of the thirty sampling schemes is shown in Table 2. Note that the error values are evaluated only for the discrete number of samples as the barycentric and RBF interpolations operate on the 30 predefined sampling schemes. The average MRE (over all the materials and schemes) of the barycentric interpolation is almost 7.5-times as high as for the BRDF slices. The RBF achieves better performance, but its average MRE is still almost 3.9-times higher than the MRE of the BRDF slices.

Figure 5 shows the progression of the reconstruction error as a function of the number of samples for all tested methods with two materials. The convergence of the proposed algorithm to low MRE values as a function of the count of samples is very fast (see green line in Fig. 5). While the RBF method performs well for lower numbers of samples, the proposed method has a superior performance relative to higher numbers of samples. When the count of samples is over 5,000, our method achieves high quality results that are significantly better than those achieved using uniform interpolation methods. In Figure 6, we show comparison of all three methods with the reference rendering for two materials and 8,911 reciprocal samples. We use the *grace* environment represented by means of 256 lights. Our method provides the best reproduction of the specular and the anisotropic highlights.

Practical Measurement Experiment – The previous experiment was performed using the reference BRDFs represented by an analytical model. However, this sacrifices some visual features of the original reflectance behavior that cannot be reliably represented by the model. Therefore, we perform practical BRDF measurement experiments collecting 8,911 samples. First, we record these samples uniformly (sampling scheme 14, see the supplementary material) and interpolate them using the barycentric and RBF interpolations. Then, we record the same count of samples adaptively using the proposed method. Altogether, we measure two datasets for each of the three materials (fabric112, fabric135, fabric136). All measurements are performed using the UTIA gonioreflectometer [FVH*13] capturing HDR RGB images of the material. The device allows for the placement of an almost arbitrary combination of illumination and viewing directions with high angular accuracy. Arm positioning and capturing of one sample, i.e. HDR RGB image, takes typically 15 seconds. Acquisition time using the adaptive method (25 hours) is about 10% longer in comparison to the uniform sampling of the same count of samples due to the data processing overhead as required by the adaptive algorithm.

We compare the data in an applied situation using a 3D scene comprised of four spheres illuminated by a single point-light source. Therefore, many combinations of illumination and view directions are covered providing a comprehensive preview of properties of the materials. The rendered images are divided into a sparse raster with only 6,195 occupied pixels representing the directions that are reachable by the gonioreflectometer; therefore, only this count of BRDF values is measured for the three materials. The entire scene is then rendered using those pixels, which we call *control samples*, and we use them as our reference. Note that pixels representing directions unreachable by the gonioreflectometer due

Table 2: *A decrease of the MRE due to usage of the proposed method instead of the barycentric interpolation (fist row) or the RBF interpolation (second row). Average values over 30 sampling schemes.*

	Brush. alum	Purple satin	Red velvet	Yellow satin	fabric 002	fabric 041	fabric 112	fabric 135	fabric 139	wood 01	mean
proposed vs. barycentric	5.68×	5.88×	26.40×	2.56×	6.68×	6.80×	5.06×	2.04×	4.53×	9.24×	7.49×
proposed vs. RBF	6.97×	2.21×	10.58×	1.68×	2.79×	4.48×	1.45×	1.11×	2.28×	5.07×	3.86×

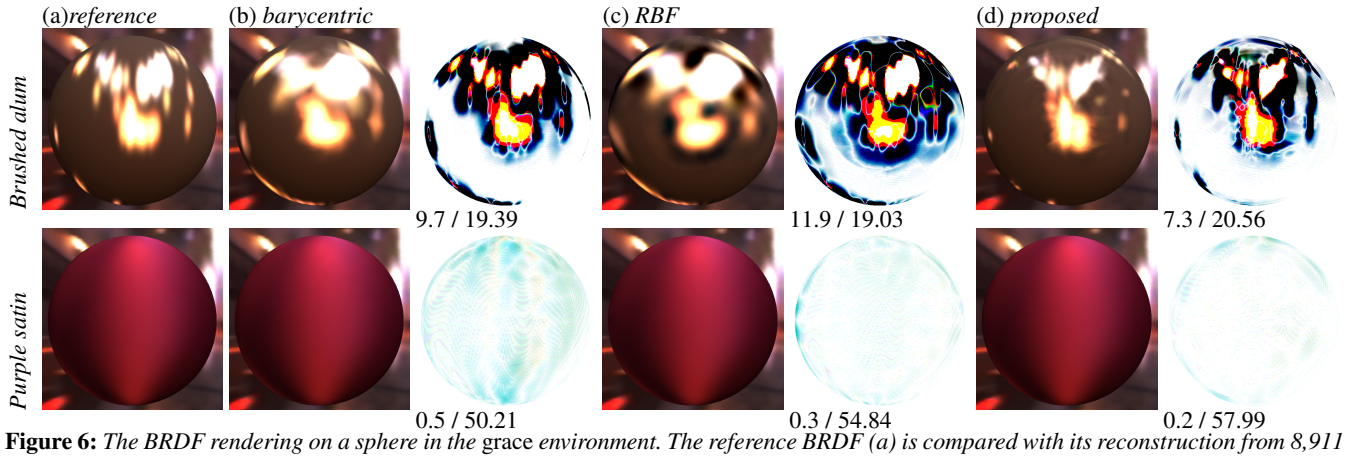

Figure 6: *The BRDF rendering on a sphere in the* grace *environment. The reference BRDF (a) is compared with its reconstruction from 8,911 samples using (b) the barycentric interpolation, (c) the RBF interpolation, and (d) the proposed method. Difference images are scaled 10× and below are difference values in CIE ΔE / PSNR [dB].*

Table 3: *The MRE [%] of the two compared adaptive method.*

	Brush. alum	Purple satin	Red velvet	Yellow satin	fabric 002	fabric 041	fabric 112	fabric 135	fabric 139	wood 01	mean
(a) our method, 8,911 samples	24.0	0.8	0.1	10.2	0.5	0.2	1.3	3.9	0.5	0.2	4.2
(b) [FVH*13], 8,911 samples	68.5	1.6	2.1	10.7	1.8	1.1	2.8	3.9	0.9	1.1	9.5
(c) our method, 18,721 samples	19.6	0.5	0.1	5.6	0.3	0.1	0.9	2.5	0.3	0.1	3.0
(d) [FVH*13], 18,721 samples	31.7	0.9	1.3	6.8	1.2	0.8	1.9	2.6	0.6	0.7	4.9

to occlusion of view of the camera by the light source are not included into the *control samples* (resulting into white spot in the difference images in Fig. 7 on the most left sphere). Their values are interpolated from regular measurements for purposes of visualization. Then, we render the same scene using the values obtained by the three compared methods and evaluate their results at all *control samples*. Figure 7 shows the reference scene side-by-side its reconstruction using all tested methods. From the accompanying error values we conclude that our method achieves by far the best performance on the real BRDF data. For more results see the supplementary material. The captured data are publicly available at http://btf.utia.cas.cz.

Also, we evaluate contribution of the proposed method over [FVH*13], i.e., the horizontal and vertical slices included on the top of the axial and diagonal slices. Results of the comparison summarized in Table 3 show that our method achieves in average almost twice lower errors.

6. Discussion

Advantages of the Method – In contrast to competitive methods, the main advantage of the proposed adaptive sampling is its faster decrease of reconstruction errors in correlation with the increasing number of samples (especially for their lower counts, see Fig. 4). Thus, on average we achieve almost four times lower relative errors given the same count of samples and between two- and five-times less samples necessary to reach the same reconstruction errors. Additionally, the proposed adaptive sampling method operates along the one-dimensional slices in the BRDF space that allows data acquisition by a continuous movement of a light source and a sensor. It is especially beneficial for sequential measurement devices, e.g., gonioreflectometer-based.

Limitations of the Method – all tested methods exhibit decreasing improvement of the performance relative to the increasing number of samples approaching an asymptotic value. A reason for this behavior is lack of samples at locations representing the specular and anisotropic highlights. They are not sampled properly by the uniform sampling for the RBF and barycentric methods or by the uniform positioning of the slices in BRDF subspaces by the proposed method. We believe that the use of a better parameterization in combination with an adaptive placement of the slices would further improve the performance.

As the proposed method is designed to represent, in particular, features that are perpendicular to the slices, it can suffer from an improper representation of curved highlights or visual features occurring between the slices. Such behavior is typical for subspaces with a high difference between the viewing and illumination elevation. These errors can be suppressed by the elevation-angle dependent interpolation method [VF16a] that interpolates data along the anisotropic highlights.

Timings – Reconstruction of the entire BRDF space with a uniform step of 2^o requires about 45 seconds using the barycentric interpolation; whereas, the RBF interpolation takes about 22 min-

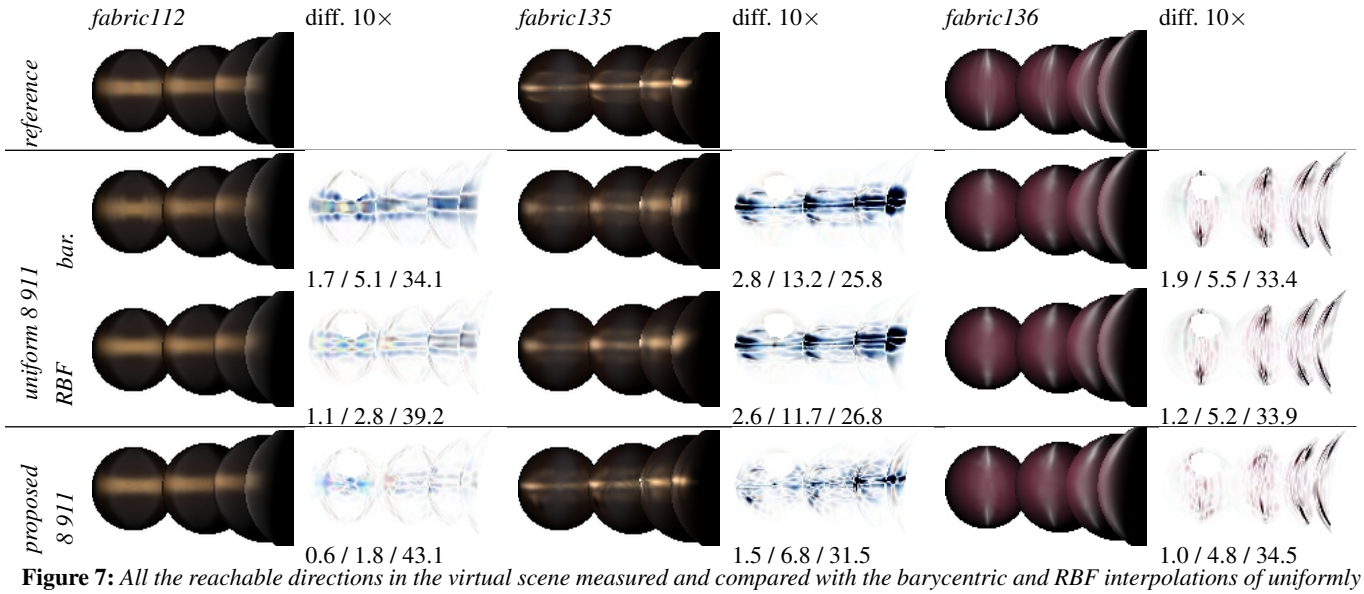

Figure 7: *All the reachable directions in the virtual scene measured and compared with the barycentric and RBF interpolations of uniformly measured data , and the proposed adaptive measurement. 8,911 samples are used, the difference values are in CIE ΔE / RMSE / PSNR [dB].*

utes, both regardless the number of samples. Reconstruction of the whole BRDF array by the proposed method using our Matlab implementation typically takes 4 minutes. All timings are obtained using a single core of Intel Xeon E5-2643 3.3 GHz.

7. Conclusions

Our paper deals with efficient sampling and reconstruction of the anisotropic BRDFs from a predefined number of samples placed along one-dimensional data slices. We compare performance of our method with the barycentric and RBF interpolation approaches. In the simulated measurement the proposed method achieves on average almost four-times lower reconstruction errors as compared to the uniform sampling combined with two interpolation methods. Alternatively, for a given reconstruction error, our method requires between two- to five-times less samples than the competing approaches. In the real measurement of the anisotropic BRDFs, our method achieves a twice lower reconstruction error than other approaches and our further experiments suggest that the captured BRDF data belong among the best publicly available anisotropic BRDFs. We have also verified that the proposed method performs almost twice better than the previous adaptive method [FVH*13].

Acknowledgments

This research has been supported by the Czech Science Foundation grant 17-02652S.

References

[Boo89] BOOKSTEIN F. L.: Principal warps: thin-plate splines and the decomposition of deformations. *IEEE TPAMI 11*, 6 (1989), 567–585. 2

[Cox69] COXETER H. S. M.: *Introduction to Geometry*. New York: Wiley, 1969. 2, 4

[FBLS07] FUCHS M., BLANZ V., LENSCH H. P., SEIDEL H.-P.: Adaptive sampling of reflectance fields. *ACM Trans. Graph. 26*, 2 (June 2007), 1–18. 2

[Fil12] FILIP J.: Restoring illumination and view dependent data from sparse samples. In *the 21th International Conference on Pattern Recognition, ICPR 2012* (2012), pp. 1391–1394. 2

[FVH*13] FILIP J., VAVRA R., HAINDL M., ZID P., KRUPICKA M., HAVRAN V.: BRDF slices: Accurate adaptive anisotropic appearance acquisition. In *CVPR 2013* (2013), pp. 4321–4326. 1, 2, 3, 4, 5, 6

[KSKK10] KURT M., SZIRMAY-KALOS L., KŘIVÁNEK J.: An anisotropic BRDF model for fitting and monte carlo rendering. *SIGGRAPH Comput. Graph. 44* (2010), 3:1–3:15. 3

[LLSS03] LENSCH H. P., LANG J., SÁ A. M., SEIDEL H.-P.: Planned sampling of spatially varying BRDFs. *Computer Graphics Forum 22*, 3 (2003), 473–482. 2

[MPM03] MATUSIK W., PFISTER H.P. BRAND M., MCMILLAN L.: Image-based BRDF measurement including human skin. In *Proc. of 10th Eurographics Workshop on Rendering* (2003), pp. 139–152. 2

[NDM05] NGAN A., DURAND F., MATUSIK W.: Experimental analysis of BRDF models. In *Eurographics Symposium on Rendering 2005* (2005), pp. 117–126. 3

[NFM14] NAUYOKS S. E., FREDA S., MARCINIAK M. A.: Dynamic data driven bidirectional reflectance distribution function measurement system, 2014. 2

[NJR15] NIELSEN J. B., JENSEN H. W., RAMAMOORTHI R.: On Optimal, Minimal BRDF Sampling for Reflectance Acquisition. *ACM Trans. Graph. (TOG) 34*, 6 (Oct. 2015), 186:1–186:11. 2

[NKS14] NÖLL T., KÖHLER J., STRICKER D.: Robust and accurate non-parametric estimation of reflectance using basis decomposition and correction functions. In *ECCV (LNCS 8690)* (2014), pp. 376–391. 2

[NRH*77] NICODEMUS F., RICHMOND J., HSIA J., GINSBURG I., LIMPERIS T.: Geometrical considerations and nomenclature for reflectance. *NBS Monograph 160, U.S. Dept. of Com.* (1977), 1–52. 1

[PTVF92] PRESS W. H., TEUKOLSKY S. A., VETTERLING W. T., FLANNERY B. P.: *Numerical Recipes in C: The Art of Scientific Computing*. Cambridge University Press, 1992. 1, 4

[VF16a] VAVRA R., FILIP J.: BRDF interpolation using anisotropic stencils. In *Proceedings of IS&T Electronic Imaging* (2016), pp. 1–6. 5

[VF16b] VAVRA R., FILIP J.: Minimal Sampling for Effective Acquisition of Anisotropic BRDFs. *Computer Graphics Forum (Pacific Graphics 2016)*, 7 (2016), 299 – 309. 2

[WKB14] WARD G., KURT M., BONNEEL N.: Reducing anisotropic BSDF measurement to common practice. In *Proceedings of the MAM* (2014), pp. 5–8. 2